

Quaternion MIMO Millimeter Wave Antenna for 5G Applications

Ming Ming Gao^{1, 2}, Jun Wang^{1, *}, Jing Chang Nan¹, and Hong Liang Niu¹

Abstract—In order to reduce the multipath fading caused by the reflection of various obstacles in short-distance communication, this paper designs a quaternion MIMO millimeter wave antenna working at 28 GHz. The antenna design adopts an inverted trapezoidal radiation patch and a slotted trapezoidal ground plate structure, so that the $|S_{11}|$ of the antenna is lower than -10 dB in the frequency band of $24 \sim 32$ GHz. By using a 1×2 array structure as the unit of MIMO antenna, the gain of the antenna at 28 GHz is 7.5 dBi. The isolation degree of each port is lower than -25 dB by orthogonal placement of each unit. The performance of the antenna is tested by the physical production test. The actual test results show that the operating bandwidth of the antenna is consistent with the simulation results. The gain at 28 GHz is slightly lower than the simulation results by 0.1 dBi, and the isolation of each port is lower than -18 dB, which is 7 dB away from the simulation results but still meets the requirement of -15 dB for MIMO communication. The measured results show that the antenna can be used in MIMO short-distance communication system.

1. INTRODUCTION

In today's 5G era, with the rise of a large number of 5G base stations and the gradual improvement of 5G service promotion [1], 5G has a higher level of demand for data traffic transmission rate [2]. Therefore, to achieve large-scale data exchange, the introduction of multiple input multiple output (MIMO) technology has become the focus of 5G technology development [3]. MIMO antenna relies on its diversity characteristics to establish multiple independent transmission paths, which can transmit the same information at the same time, so as to ensure that even if a signal will be deeply weakened during transmission, it will still receive a strong signal at the receiving end [5]. The previous four generations of mobile communication usually use a relatively rich sub-6 frequency band [6]. However, due to the progress of communication technology, the sub-6 frequency band has become very crowded, so transferring the 5G communication frequency band to the millimeter wave frequency band has become a research focus [7]. In July 2016, the Federal Communications Commission of the United States specified $27.5 \sim 28.35$ GHz, 37 GHz ~ 38.6 GHz, 38.6 GHz ~ 40 GHz as the frequency bands for 5G applications [8], and allocated 64 GHz ~ 71 GHz unauthorized spectrum [9]. As an important basis for the development of 5G technology, the importance of millimeter wave band is self-evident. A millimeter band four port MIMO antenna array for 5G application is proposed in [10]. The feed network of antenna is composed of a T-type power distributor. The array element is a rectangular slot patch antenna, and the floor is made of rectangular, circular, and serrated slot structures to enhance the radiation characteristics of the antenna. The working bandwidth of the antenna is $25.5 \sim 29.6$ GHz; the isolation of each port is lower than -10 dB through orthogonal placement; and the antenna gain is 8.3 dBi. Reference [11] proposed a millimeter wave array MIMO antenna, which reduced the coupling between ports by vertically adding through holes to DRA elements at appropriate locations. The

Received 17 October 2022, Accepted 28 December 2022, Scheduled 9 January 2023

* Corresponding author: Jun Wang (1024833528@qq.com).

¹ School of Electronics and Information Engineering, Liaoning University of Engineering, Huludao 125105, China. ² School of Information Science and Technology, Dalian Maritime University, Dalian 116026, China.

working bandwidth of the antenna was 24.5 ~ 27.5 GHz; the isolation of each port was less than -30 dB; and the antenna gain was 6.7 dBi. Literature [12] proposed a miniaturized MIMO antenna. By designing the EGB structure, the isolation of each port of the antenna was lower than -23 dB as a whole; its operating frequency band was 26.5 ~ 29.5 GHz; and its gain was 7 dBi. On the whole, the current millimeter wave MIMO antenna has a shortage of narrow bandwidth.

In this paper, a quaternion MIMO millimeter wave antenna is designed, which adopts an inverted trapezoidal radiation patch and a slotted trapezoidal ground plate structure, and achieves the purpose of 8 GHz long bandwidth. By using a 1×2 array structure as the unit of MIMO antenna, the purpose of higher gain is achieved. By orthogonal placement of each unit, the purpose of self-decoupling to reduce the coupling of each port is achieved. Aiming at the phenomenon that millimeter waves encounter various obstacles to reflect and cause multipath transmission during short-distance transmission, the designed antenna has the application of reducing the influence of multipath fading. $|S_{11}|$ of the designed antenna is lower than -10 dB in the frequency band of 24 ~ 32 GHz, and the isolation of each port is lower than -25 dB. The gain of the antenna is 7.5 dBi at 28 GHz. Compared with most existing millimeter-wave MIMO antennas, the bandwidth of this antenna is improved.

To compare antenna performance, Table 1 shows the performance comparison results between the millimeter wave MIMO array antenna designed in this paper and other literature antennas. Compared with [10], the antenna designed in this paper is an omnidirectional antenna, so its gain is 1.7 dBi lower than that of the directional antenna used in literature, but its isolation and bandwidth are far better than those in literature, and the antenna designed in this paper has a smaller size. Compared with [13], the gain is not much different, but the bandwidth of antenna in this paper is increased by 2 GHz. As the number of antenna ports in this paper is doubled, the mutual interference among ports becomes more, so the isolation is slightly lower. Compared with [14], because the number of selected units in the literature is twice as many as that in this paper, and the distance between two ports is far, the gain is 40% lower, the isolation is 22 dB lower, but the bandwidth is 7 GHz higher, which improves the range of applicable scenes. Compared with [11], the isolation of the antenna in this paper is lower than that in [11], but the gain is higher than that in [11] by 1 dBi, and the bandwidth is higher than that in [11], which improves greatly in general. Compared with [12], the antenna designed in this paper is superior to the reference index in terms of bandwidth (increased by 5 GHz), isolation (increased by 3 dB), and gain (increased by 0.6 dBi). Compared with reference [15], the antenna unit in this paper is an omnidirectional antenna, and [15] uses a directional antenna, so the gain is 2.2 dBi lower than that in [15], but the working bandwidth of the antenna in this paper is 3 GHz larger than that in [15], and its size is 22% smaller than that in [15]. Generally speaking, compared with the traditional MIMO antenna, the antenna designed in this paper greatly improves the gain of the antenna by using an array antenna as the unit antenna of the MIMO antenna. Compared with the same type of MIMO antenna with the same number of units, the antenna designed in this paper is far superior to the antennas in other references in terms of bandwidth and size when the gain isolation is close to each other.

Table 1. Comparison of this paper with other literature.

Literature	bandwidth	Port isolation	Gain	Unit number	ECC	DG	Size
Literature [2]	25.5 ~ 29.6 GHz	-10 dB	8.3 dBi	4	< 0.06	> 9.85	30 × 35 mm ²
Literature [5]	27 ~ 33 GHz	-28 dB	8 dBi	2	< 0.005	—	24.2 × 24.2 mm ²
Literature [6]	36.7 ~ 37.4 GHz	-40 dB	12.8 dBi	2	< 0.002	> 9.993	20 × 40 mm ²
Literature [3]	24.8 ~ 27.2 GHz	-30 dB	6.7 dBi	2	—	—	17.7 × 16 mm ²
Literature [4]	26.5 ~ 29.5 GHz	-15 dB	7 dBi	2	—	—	15 × 12.7 mm ²
Literature [7]	38.8 ~ 42.9 GHz	-28 dB	9.89 dBi	4	< 0.014	—	25 × 35 mm ²
This text	24 ~ 32 GHz	-18 dB	7.6 dBi	4	< 0.004	> 9.98	26 × 26 mm ²

2. ANTENNA DESIGN

2.1. Antenna Unit Structure Design

The structural model of the antenna unit is shown in Figure 1. The antenna adopts microstrip line feed and is composed of a radiation patch, feed line, and grounding plate. The dielectric substrate adopts a Rogers RT5880 plate with relative permittivity of 2.2; the loss tangent of dielectric substrate is 0.009; the thickness of the substrate is 0.254 mm; the size of the single element substrate is $9 \times 5 \times 0.254 \text{ mm}^3$. After optimization simulation, the dimension of the antenna is shown in Table 2.

Table 2. Antenna dimensions.

Parameters	Value	Parameters	Value	Parameters	Value	Parameters	Value
L_{11}	3.83	L_{13}	1.84	W_{12}	4.23	W_{14}	1.73
W_{11}	0.75	W_{13}	1.21	L_{15}	2.7	W_{15}	2.7
L_{12}	3.21	L_{14}	1.73	L_g	5.4	W_1	5

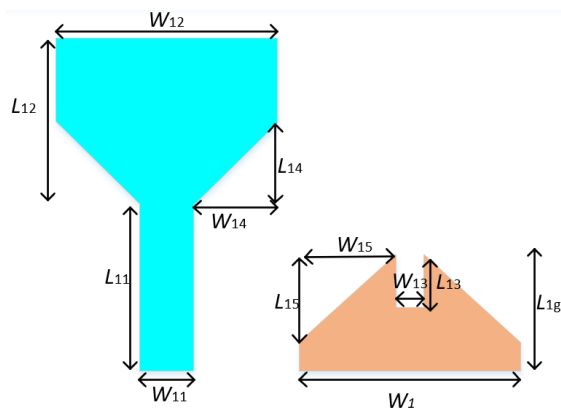


Figure 1. Antenna unit structure.

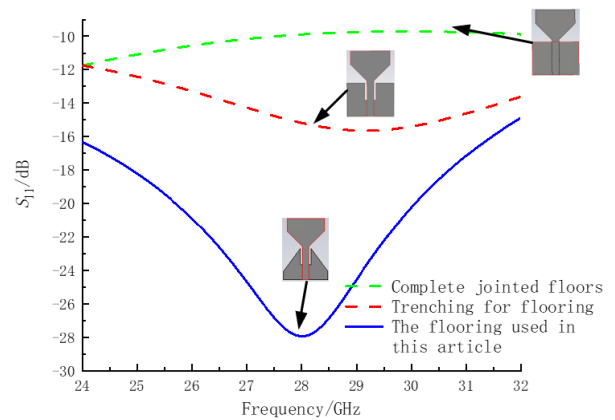


Figure 2. Effect of different grounding plates on $|S_{11}|$.

Through simulation, it is found that the ground plate has a great influence on $|S_{11}|$ of the antenna. When the antenna patch structure is determined, different shapes of ground plates are simulated, that is, complete ground plate, trenching ground plate, and the ground plate in this paper. As shown in Figure 2, it can be found that when the complete ground plate is kept, the resonance point of the antenna is far away from 28 GHz, and $|S_{11}|$ at 28 GHz is higher than -10 dB , which cannot meet the communication requirements of 28 GHz. After digging the groove in the center of the ground plate, it can be found that the resonance point of the antenna can shift to the high frequency around 28 GHz, and $|S_{11}|$ is -15.6 dB . Two corners of the ground plate used are cut off in this paper on the basis of digging the groove, and it can be found that the resonance point is at 28 GHz, and $|S_{11}|$ is lower than -10 dB at $24 \sim 32 \text{ GHz}$, which can meet the design requirements. The antenna pattern at 28 GHz is shown in Figure 3, and it can be seen that the maximum gain of the antenna is 3.9 dBi .

2.2. Single Element Array Antenna Structure Design

In order to further improve the gain of the antenna, the antenna unit is connected with one point two equal power splitter, forming a 1×2 array antenna. The antenna size is $13 \times 13 \times 0.254 \text{ mm}^3$, and its structure diagram is shown in Figure 4.

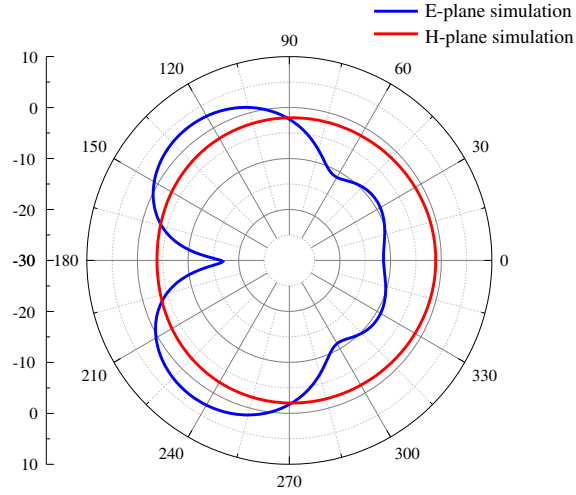


Figure 3. Pattern of antenna element at 28 GHz.

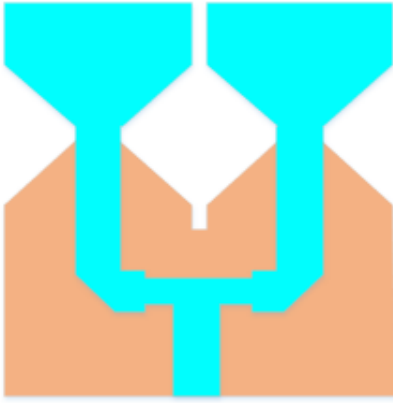


Figure 4. 1×2 array antenna structure.

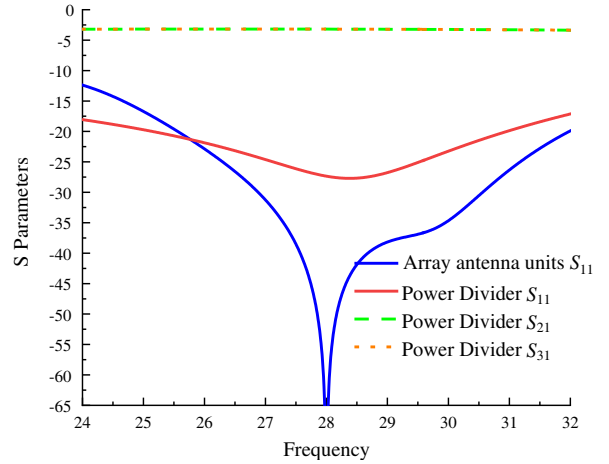


Figure 5. S -Parameters of array antenna element.

The S parameter of the power divider is shown in Figure 5. The power divider $|S_{11}|$ is below -10 dB at $24 \sim 32$ GHz, and the theoretical values of $|S_{21}|$ and $|S_{31}|$ can be obtained from formula (1), so $|S_{21}| = |S_{31}| = 10 \log_{10} \frac{1}{2} = -3$ dB, but the actual simulation result is -3.2 dB. The analysis reason is that the working frequency is too high, and the transmission line length is too long.

$$P_i = 10 \log \frac{I_i}{I_1 + I_2 + \dots + I_i} \quad (1)$$

As shown in Figure 5, $|S_{11}|$ of this array antenna element is lower than -10 dB at $24 \sim 32$ GHz, and its gain is 5.9 dBi as shown in Figure 6. It can be found that the gain is increased by 2 dBi compared with the antenna element without array, thus achieving the purpose of increasing the antenna gain.

2.3. Quaternion MIMO Antenna Structure Design

Quaternion MIMO antenna design uses polarization diversity technology. By placing each antenna element orthogonally, because the antenna elements are in orthogonal polarization state, they can only perceive the weak signals sent by each other, so as to increase the isolation of the antenna. Quad array

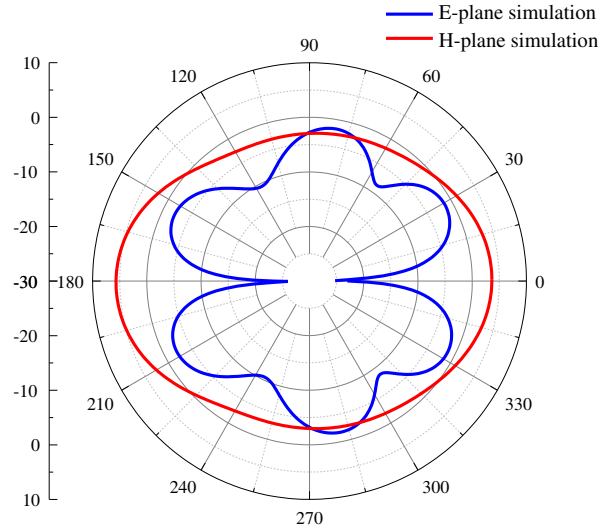


Figure 6. Pattern of array element antenna at 28 GHz.

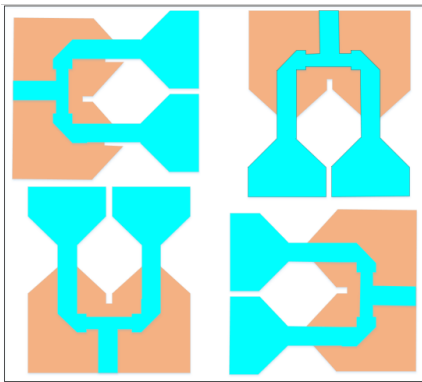


Figure 7. Structure diagram of quatern MIMO antenna.

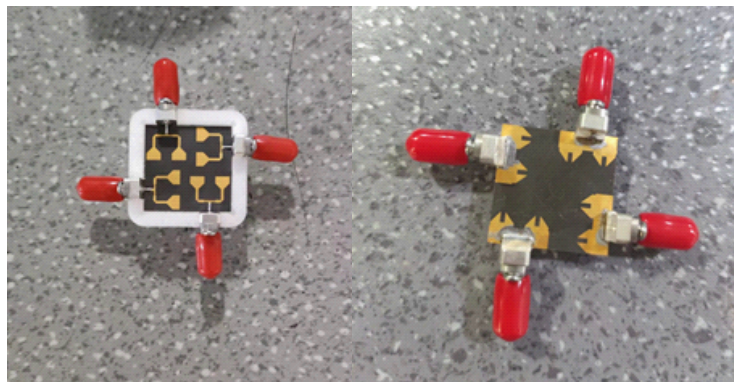


Figure 8. Antenna physical diagram.

MIMO antenna is placed clockwise by 90° on the basis of array units. The structure is shown in Figure 7, and the antenna size is $26 \times 26 \times 0.254 \text{ mm}^3$.

In order to check the performance of the designed antenna, the physical fabrication and testing were completed, and the physical picture is shown in Figure 8. The S parameters of the simulation results are shown in Figure 9. The working bandwidth of the antenna is $24 \sim 32 \text{ GHz}$, and the isolation between the antenna ports is less than -25 dB . As shown in Figure 10, the S parameter of the measured data shows that the resonating frequency of the antenna is 28.3 GHz , which is 0.3 GHz away from the expected design of 28 GHz . The operating bandwidth of the antenna is $24 \sim 32 \text{ GHz}$, which meets the simulation results of $24 \sim 32 \text{ GHz}$. The isolation of each port at 28 GHz is higher than -18 dB , of which $|S_{31}|$ and $|S_{42}|$ are 7 dB away from the simulation results of -25 dB , and other ports are similar to the simulation results. The main reason for the error between the simulation results and test results is that the connector is not put into the simulation model during the simulation, which leads to the influence of the connector on the antenna performance in the actual test. Moreover, due to the small size of millimeter wave devices, small changes in processing will affect the results. Although there is a gap between the measured and simulated results, the overall index can meet the design requirements of MIMO antenna.

Figure 11 shows the surface current distribution of the four-element MIMO array antenna simulated by HFSS software. It can be clearly seen from the figure that when only one port is excited, there is

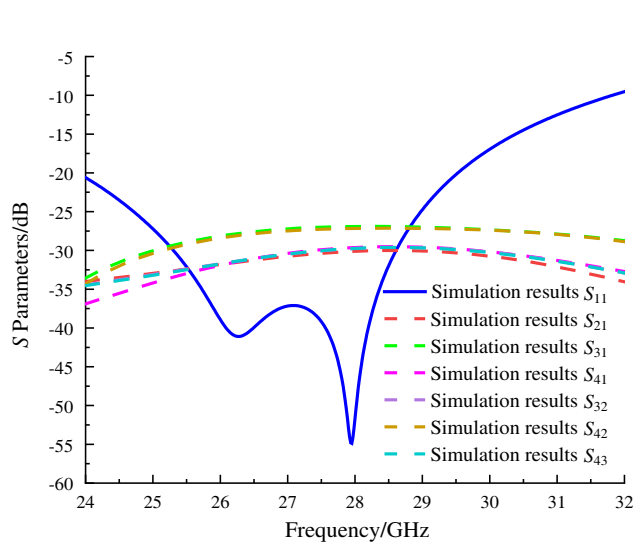


Figure 9. S -parameters of the simulated quadratic array MIMO antenna.

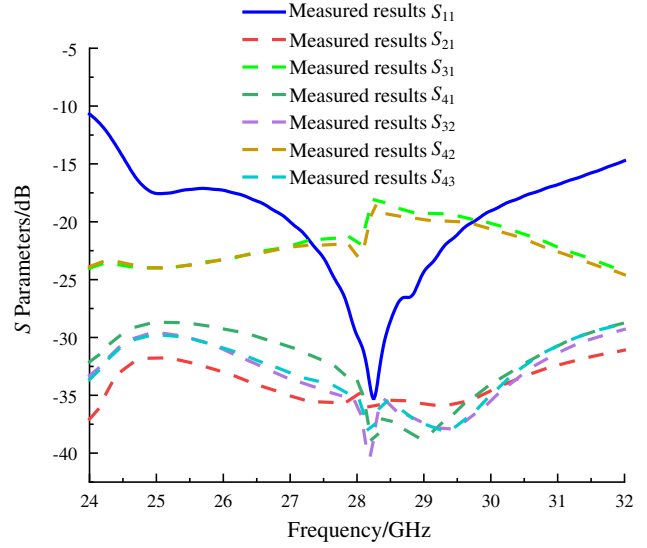


Figure 10. S -parameter plot of the measured quadratic array MIMO antenna.

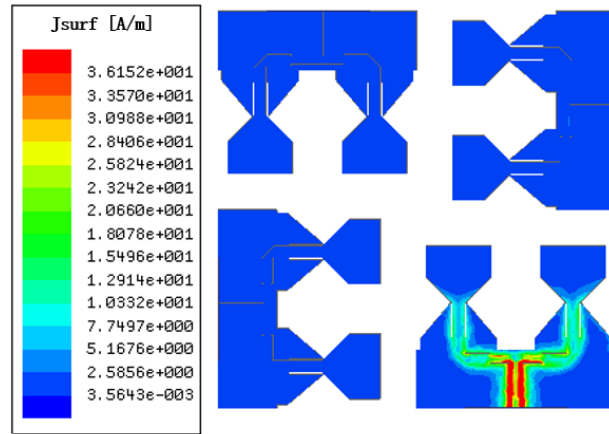


Figure 11. Antenna surface current distribution diagram.

no excessive current on the surface of the other unit, so the isolation of the antenna can be effectively improved by orthogonal placement.

3. ANALYSIS OF EXPERIMENTAL RESULTS

3.1. Radiation Properties

The simulation and measurement results of this antenna pattern are shown in Figure 12. Because each antenna element has the same structure, only one of the element ports is excited, and its patterns at 24 GHz, 28 GHz, and 32 GHz are simulated respectively. From Figure 12, it can be seen that the gain of this antenna varies slightly at different frequencies, but the maximum radiation direction is basically the same, and the pattern is basically stable in general. Measurement results of gain are slightly lower than the simulation ones, and the radiation direction is basically consistent with the simulation results.

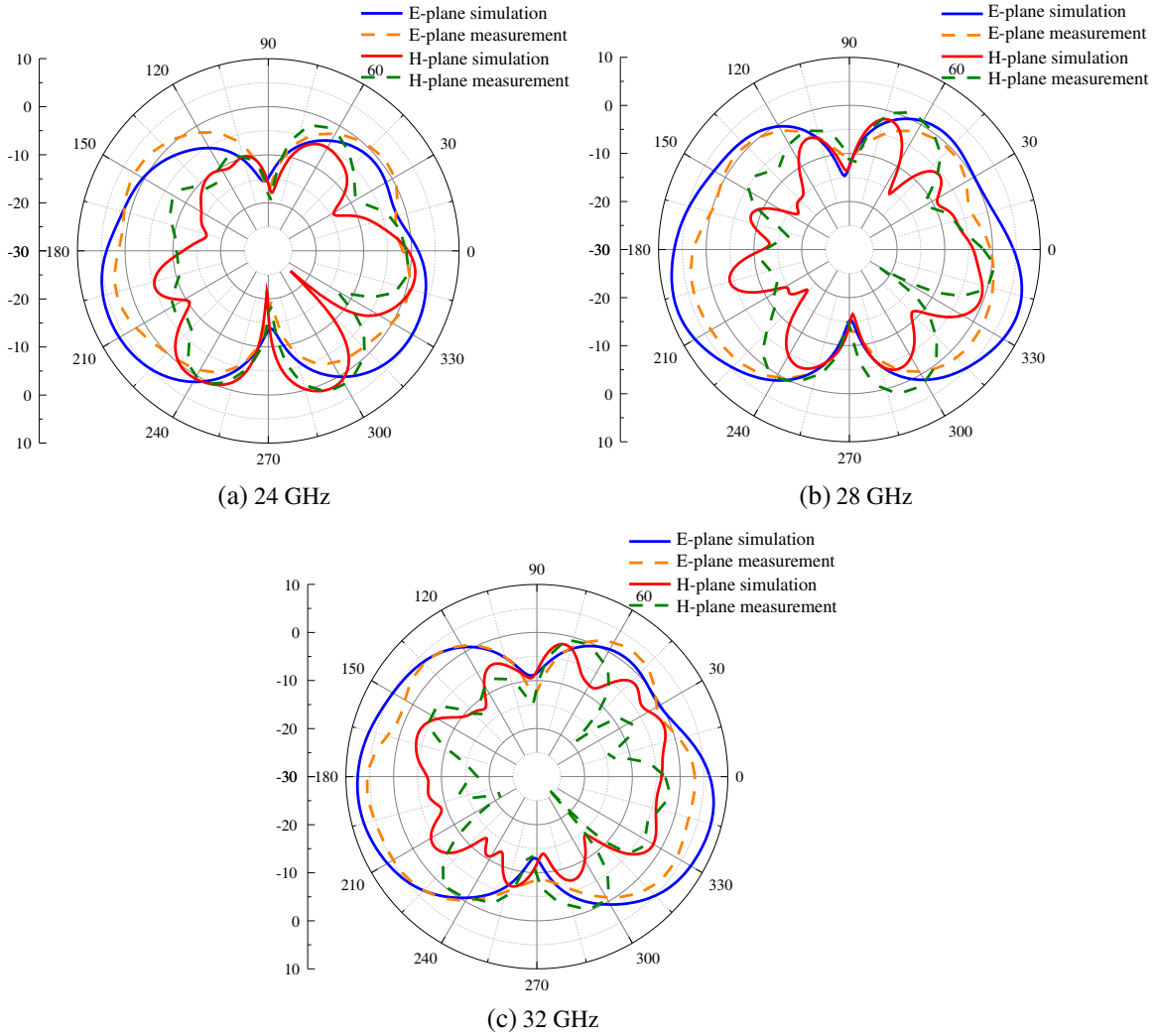


Figure 12. Comparison between directional simulation and actual measurement.

3.2. Gain Analysis

See Figure 13 for the comparison results between the simulated and measured antenna gains. In the actual measurement, the antenna gain range is 6.15 ~ 7.6 dBi, which is slightly lower than the simulated 6.17 ~ 7.78 dBi. The difference between the two is 0.2 dBi, and the measured antenna gain reaches 7.45 dBi at 28 GHz, which is 0.1 dBi lower than the simulated 7.5 dBi.

3.3. Diversity Characterisation

The diversity performance of a MIMO antenna can be measured by the diversity gain (DG) and envelope correlation coefficient (ECC) of the antenna. The ECC and DG are calculated as in Equation (2) and Equation (3) and shown in

$$ECC = \frac{|S_{11}^* S_{12} + S_{21}^* S_{22}|^2}{(1 - |S_{11}|^2 - |S_{21}|^2)(1 - |S_{22}|^2 - |S_{12}|^2)} \tag{2}$$

$$DG = 10\sqrt{1 - |ECC|^2} \tag{3}$$

Figure 14 shows ECC and DG parameters of the antenna. As can be seen from the figure, ECC

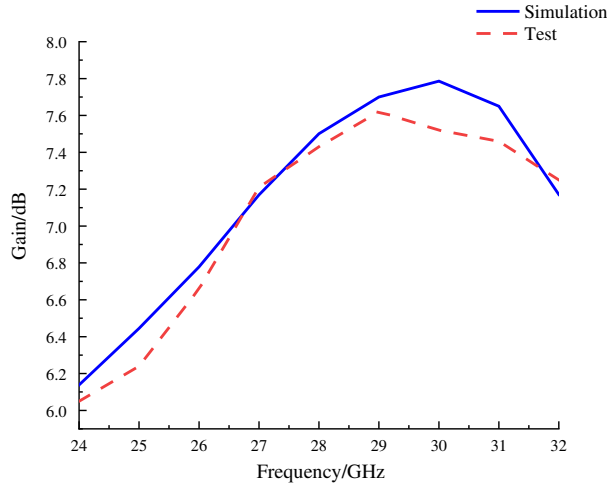


Figure 13. Measured gain and comparison chart.

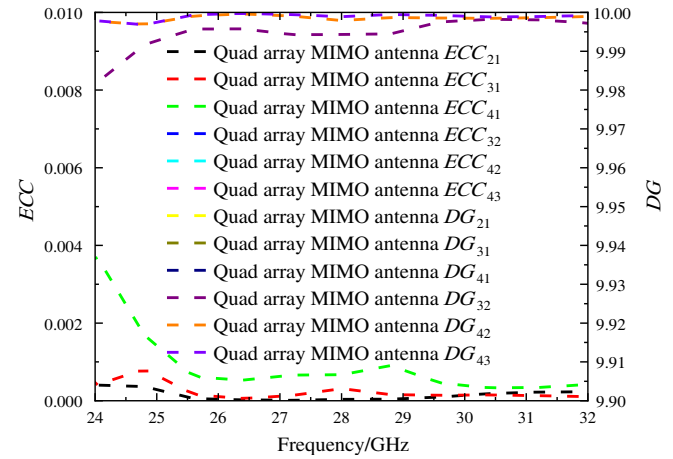


Figure 14. Quad array MIMO antenna ECC and DG .

parameters of the antenna are all less than 0.004, which is far less than the required 0.5. In addition, DG parameters of the antenna are all greater than 9.98 dB.

4. CONCLUSION

In this paper, a quaternion MIMO millimeter wave antenna is designed. The bandwidth of the antenna is 24 ~ 32 GHz. By placing the antenna elements orthogonally, the isolation between the ports is less than -25 dB. At the same time, the gain of the antenna can reach 7.78 dBi by using a 1×2 array antenna as the unit of the MIMO antenna. The actual test shows that the operating bandwidth of the antenna accords with the simulation results. The gain at 28 GHz is 0.1 dBi lower than the simulation results, and the isolation is 7 dB lower than the simulation results, but it is still lower than the -15 dB required by MIMO antenna. Generally speaking, the antenna can be used in short-distance wireless communication, effectively reducing the debilitating influence caused by multipath transmission.

DATA AVAILABILITY

The datasets used and/or analysed during the current study are available from the corresponding author on reasonable request.

ACKNOWLEDGMENT

1. Liaoning Applied Basic Research Project: Design and Research of 5G Millimeter Wave Array Antenna (22-1083).
2. National Fund: Research on Power Amplifier Design Modeling and Predistortion of Cognitive Radio System under Compressed Sensing Framework (61701211).
3. General Program of National Natural Science Foundation of China: Research on Modeling of Future-Oriented Reconfigurable Radio Frequency Module and Neural Network (61971210).
4. Liaoning Applied Basic Research Program (2022JH2/101300275).

REFERENCES

1. Subitha, D., S. Velmurugan, M. Vanitha Lakshmi, P. Poonkuzhali, T. Yuvaraja, and S. Alemayehu, "Development of Rogers RT/Duroid 5880 substrate-based MIMO antenna array for automotive radar applications," *Materials Science and Engineering*, Vol. 11, 2022.

2. Khalid, M., X. Qin, Y. X. Sun, et al., "4-Port MIMO antenna with defected ground structure for 5G millimeter wave applications," *Electronics*, Vol. 9, 71, 2020.
3. Pan, Y. M., X. Qin, Y. X. Sun, and S. Y. Zheng, "A simple decoupling method for 5G millimeter-wave MIMO dielectric resonator antennas," *IEEE Transactions on Antennas and Propagation*, Vol. 67, No. 4, 2224–2234, 2019.
4. Shen, X., Y. Liu, L. Zhao, and G.-L. Huang, "A miniaturized microstrip antenna array at 5G millimeter wave band," *IEEE Antennas and Wireless Propagation Letters*, Vol. 18, No. 8, 1671–1675, 2019.
5. Wani, Z., M. P. Abegaonkar, and S. K. Koul, "Dual-beam antenna for millimeter wave MIMO applications," *2018 IEEE Indian Conference on Antennas and Propagation (InCAP)*, 1–3, 2018.
6. Khan, J., S. Ullah, U. Ali, F. A. Tahir, I. Peter, and L. Matekovits, "Design of a millimeter-wave MIMO antenna array for 5G communication terminals," *Sensors*, Vol. 22, 2768, 2022.
7. Manan, A., S. I. Naqvi, M. A. Azam, Y. Amin, J. Loo, and H. Tenhunen, "MIMO antenna array for mm-wave 5G smart devices," *22nd International Multitopic Conference (INMIC)*, 1–5, 2019.
8. Rajkumar, S., A. Anto Amala, and K. T. Selvan, "Isolation improvement of UWB MIMO antenna utilising molecule fractal structure," *Electronics Letters*, Vol. 55, No. 10, 576–579, 2019.
9. Chithradevi, R. and B. S. Sreeja, "A compat UWB MIMO antenna with high isolation and low correlation for wireless applications," *2017 IEEE International Conference on Antenna Innovations & Modern Technologies for Ground, Aircraft and Satellite Applications (IAIM)*, 1–4, 2017.
10. Manage, P. S., U. Naik, S. Kareemulla, and V. Rayar, "Dual band notched UWB-MIMO antenna incorporating CSRR for WLAN and X band applications," *2020 Third International Conference on Smart Systems and Inventive Technology (ICSSIT)*, 149–152, 2020.
11. Banerjee, J., R. Ghatak, and A. Karmakar, "A compact planar UWB MIMO diversity antenna with Hilbert fractal neutralization line for isolation improvement and dual band notch characteristics," *2018 Emerging Trends in Electronic Devices and Computational Techniques (EDCT)*, 1–6, 2018.
12. Liu, Y., X. Yang, Y. Jia, and Y. J. Guo, "A low correlation and mutual coupling MIMO antenna," *IEEE Access*, Vol. 7, 127384–127392, 2019.
13. Zhou, X., H. Zhai, L. Xi, Z. Wei, Z. Ma, and L. Zheng, "A low-profile four-element MIMO antenna array with new decoupling structures," *Microw. Opt. Technol. Lett.*, Vol. 60, 2511–2516, 2018.
14. Chang, L., Y. Yu, K. Wei, and H. Wang, "Orthogonally polarized dual antenna pair with high isolation and balanced high performance for 5G MIMO smartphone," *IEEE Transactions on Antennas and Propagation*, Vol. 68, No. 5, 3487–3495, 2020.
15. Sufian, M. A., N. Hussain, H. Askari, S. G. Park, K. S. Shin, and N. Kim, "Isolation enhancement of a metasurface-based MIMO antenna using slots and shorting pins," *IEEE Access*, Vol. 9, 73533–73543, 2021.